Global Solution of Economic Dispatch with Valve Point Effects and Transmission Constraints

Loïc Van Hoorebeeck
P.-A. Absil
ICTEAM Institute
UCLouvain
Louvain-la-Neuve, Belgium
loic.vanhoorebeeck@uclouvain.be

Anthony Papavasiliou
Center for operations research and econometrics
UCLouvain
Louvain-la-Neuve, Belgium

***Abstract*—Gas units are becoming an increasingly important component of modern power system operations, due to the flexibility that they offer in a regime of large-scale renewable energy integration. The valve point effect refers to the loss of efficiency when operating a turbine off a valve point, that is just after the previous valve opens. The valve point effect for gas power plants is a primary attribute of their operation, however its representation raises computational challenges, due to the non-convex and non-smooth model that is required for representing the fuel cost. In this work, a new heuristic based on successive piecewise approximations of the cost function is described. This heuristic consists in two steps: first, the optimization is run over the whole feasible set and a lower bound for the optimal objective is obtained, then the feasible solutions collected in the previous step are enhanced through local searches. The approach is tested on several IEEE bus systems that have been extended with generators obeying a valve point effect.**

***Index Terms*—Economic dispatch, global optimization, mixed-integer programming, non-convex optimization, non-smooth optimization.**

I. Introduction

Gas units are gaining importance as components of modern power system operations, as a result of the adaptability that they offer in systems with significant levels of renewable energy integration. Various market operators, such as the Midcontinent ISO, have made some advances in the representation of detailed and complex operating and cost constraints of gas units in their unit commitment and economic dispatch models. The focus of the present paper is the valve point effect (VPE) in the context of a multi-period economic dispatch model, which serves as a starting point for the modelling of this important operational attribute in more advanced operational planning models.

Commonly, fuel costs in economic dispatch are modelled as smooth quadratic functions. Such convex models do not account for the valve point loading effect: a turbine which is loaded at a valve point, i.e., just before the next valve opens, operates at full efficiency and a turbine operating off a valve point is working less efficiently due to throttling losses [1]. This effect significantly alters the output of gas units. A typical model for a fuel cost function that accounts for the valve point effect is the sum of a quadratic component with a non-smooth and non-convex rectified sine function, as detailed in eq. (5). The operational constraints of the considered problem include power-range restrictions and ramp constraints. We further consider transmission constraints, which are represented using the DC optimal power flow model.

While the valve point effect has been accounted for in various economic dispatch models in the literature (see, e.g. [2], [3], [4]), few studies investigate its impact in the context of optimal power flow (OPF) such as [5]. Besides, most approaches are based on heuristics and do not show any guarantees with respect to the optimality of the returned solution. In [6], a globally convergent method relying on piecewise-quadratic approximations was developed. This method was extended in [7] to multi-periodic cases but suffers from a long execution time.

In this work, we extend this approach to handle network constraints, and in order to remedy the long execution time, we describe a heuristic able to capture solutions of similar quality in a reduced amount of time. We demonstrate the effectiveness of our proposed heuristic in a transmission-constrained IEEE network, and illustrate the notable impact of accounting for the valve point effect in systems with significant levels of gas unit integration: the valve point effect substantially affects the dispatch, and neglecting it can lead to significant short-term operational efficiency losses. These methods can be easily extended to more complicated models that include spinning reserves, multiple fuels and prohibited operating zones.

The approach followed here, and introduced in [6], [7], can be summarized as follows. First a piecewise linear or quadratic under-approximation of the non-smooth and non-convex cost functions is constructed around a chosen set of knots, where the knots refer to the points where the pieces meet. This new objective function, as well as the operational and transmission constraints of the problem, constitute the initial surrogate economic dispatch problem. This surrogate problem is then fed into a mixed-integer programming solver, e.g., Gurobi, which

returns a solution along with a lower bound to the global objective. As the feasible set of the problem is represented exactly, any solution of the surrogate problem is feasible for the true problem. Moreover, any lower bound of the surrogate economic dispatch model is a valid lower bound of the economic dispatch problem, because the surrogate problem works with an under-approximation of the actual problem that we wish to solve. Hence, an interval in which the globally optimal cost of the economic dispatch problem must lie, is obtained. If the prescribed tolerance is not met, the solution of the surrogate economic dispatch problem is added to the set of knots. This defines a new piecewise objective which is in any point superior or equal to the first surrogate function. The algorithm stops either when the target tolerance is attained, or when the surrogate function matches the true function at the optimum of the former. In this way, any tolerance up to the solver accuracy can be attained.

The structure of the paper is as follows. In section II the main and surrogate problems are introduced. The global method is described in section III, and two versions of a heuristic are defined. Then, the method and both heuristics are tested on two IEEE test systems in section IV. Finally conclusions are drawn in section V.

II. Mathematical formulation of DED-DCOPF

A. Main problem: DCOPF based on reactance

We employ a bus angle model of the DC optimal power flow (DCOPF) problem, where the network is described as an oriented graph. The parameter B_k corresponds to the reactance of a line $k = (m, n)$. The flow of power, e_{kt}, along line k at time t, is then described as a function of the bus angle difference along the nodes that the line is joining:

$$e_{kt} = B_k(\theta_{mt} - \theta_{nt})\,, \tag{1}$$

where θ_{mt} stands for the angle of the voltage phasor of bus m at time step t. We fix the angle of the reference bus (indexed by 0), i.e., $\theta_{0t} = 0$ for all t. If losses are neglected, the main addition to the common economic dispatch models, that are employed in the literature for accounting for the valve point effect, is in the power balance constraint:

$$-\sum_{g\in G_n} p_{gt} - \sum_{k=(\cdot,n)} e_{kt} + D_{nt} + \sum_{k=(n,\cdot)} e_{kt} = 0\,. \tag{2}$$

where G_n is the set of generators at bus n and D_{nt} the demand of bus n at time t.

This constraint must hold for each bus n, and in the multi-period case, for each time period t. Given a flow limit TC_k for line k, the flow of power along each line is constrained as follows:

$$-TC_k \le e_{kt} \le TC_k\,. \tag{3}$$

With these three additional constraints, the dynamic economic dispatch (DED) problem studied in [7] can be readily extended as the minimization of the non-convex and non-smooth objective,

$$\text{(DED-DCOPF)} \qquad \min \sum_{t\in T}\sum_{g\in G} f_g(p_{gt})\,, \tag{4}$$

with cost functions [8],

$$f_g(p_{gt}) = \underbrace{A_g p_{gt}^2 + B_g p_{gt} + C_g}_{:=f_g^{\mathrm{Q}}(p_{gt})} + \underbrace{D_g\ \left|\sin E_g(p_{gt} - P_g^-)\right|}_{:=f_g^{\mathrm{V}}(p_{gt})}\,. \tag{5}$$

Here, p_{gt} represents the production of generator g at time t; A_g, B_g, C_g, D_g, E_g correspond to cost parameters, and P_g^- is the minimum operating range of the plant. The following constraints apply:

- Power generation restrictions

$$P_g^- \le p_{gt} \le P_g^+\,, \tag{6}$$

- Ramp rate limits

$$R_g^- \le p_{gt} - p_{g(t-1)} \le R_g^+\,, \tag{7}$$

- Flow constraints, eqs. (1) to (3).

In these constraints, P_g^+ is the max power generation limits of unit g, and R_g^- and R_g^+ are the lower and upper ramp limits, respectively. Note that the angles at each bus, θ, and the flows over each line, e, can be fully determined from the production at each node n. For the sake of simplicity, the main problem (DED-DCOPF) is denoted as (P) in the following. The surrogate problem, introduced hereafter, is denoted as (S).

B. Surrogate problem

Due to the linearization of the flow constraints via the DCOPF model, the feasible set of (P) is a polyhedron and the main difficulty in solving the problem comes from the non-convex and non-smooth objective. Thus, in a similar fashion as [6], a surrogate problem (S) is defined by approximating the objective without changing the feasible set, namely by employing the following objective function:

$$\text{(S)} \qquad \min \sum_{t\in T}\sum_{g\in G} h_{gt}(p_{gt})\,, \tag{8}$$

subject to the constraints of eqs. (1) to (3), (6) and (7).

Given the set of knots $\boldsymbol{X}_{gt} := \left(X_{gt1}, \ldots, X_{gtn_{gt}^{\mathrm{knot}}}\right)$, the terms of eq. (8) read as

$$h_{gt}(p_{gt}) := \begin{cases} \hat{f}_g(p_g\,;\boldsymbol{X}_{gt}) & \text{if } f_g^{\mathrm{V}} \neq 0\,, \\ f_g^{\mathrm{Q}}(p_g) & \text{else.} \end{cases} \tag{9}$$

Here, $\hat{f}(\bullet\,;\boldsymbol{X})$ stands for the piecewise-linear interpolation of f, given the knots $\boldsymbol{X}$. The smooth part of the objective, f_g^{Q}, and the non-smooth part, f_g^{V}, are defined as in eq. (5).

Fig. 1 depicts the main and surrogate objective for a given unit g and time step t. The initial objective, f_g, is plotted in solid line and the smooth part, f_g^{Q}, in dash-dotted line. The points where both curves meet are the points at which the sine from the non-smooth part, f_g^{V},

vanishes and therefore at which the initial objective is not smooth due to the absolute value in eq. (5). We refer to these points as *kink points*. As explained in section III, the approach considered here consists in successively adding knots to the piecewise approximation to refine it. These knots, $\boldsymbol{X}_{gt}^k$, which define the piecewise approximation, h_{gt}^k, at step k of the algorithm are depicted as bullets and include the kink points. The colour difference illustrates when the points were added to the set of knots: the red ones belong to the initial set of knots, the green have been added during previous iterations and the purple is the – possibly inexistant – knot to be added. Let us now consider the choice of initial knots and the monotonic property of two successive approximations.

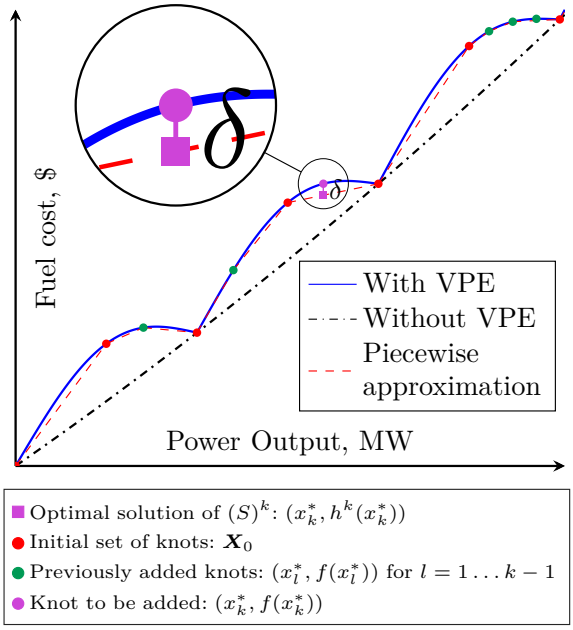

Fig. 1. Illustration of the method APLA at iteration k on a single term of the objective.

1) Choice of the initial knots: In order for the interpolant to be lower than the original function that we wish to approximate, it can be shown that the kink points should be included in the set of knots [7]. However, this gives a poor initial approximation: the interpolant being the zero function. Indeed, since f_g^{V} vanishes at the kink points, $\boldsymbol{X}^{\mathrm{kink}}$, we have $\hat{f}_g^{\mathrm{V}}(p_g\,;\boldsymbol{X}^{\mathrm{kink}}) = 0$ for all p_g. Therefore, the maxima of f_g^{V} are also added to the initial set, $\boldsymbol{X}_{gt}^0$. This gives the red dots of Fig. 1.

2) Monotonic property: If f_g is piecewise-concave between two kink points, we have

$$\boldsymbol{X}^1 \subseteq \boldsymbol{X}^2 \implies \hat{f}_g(p_g\,;\boldsymbol{X}^1) \leq \hat{f}_g(p_g\,;\boldsymbol{X}^2) \leq f_g(p_g) \quad (10)$$

given any feasible point p_g and set of knots $\boldsymbol{X}^1$ containing the kink points of f_g.

The novel aspect of the present paper relative to [7] is the addition of the network constraints, as well as the development of heuristics which reduce the execution time and avoid timeouts. The comparison of the different methods in section IV shows that the heuristics reach comparable solution in a significantly reduced execution time.

III. Methods

This section is devoted to the description of two methods. The first one (section III-A) is largely similar to the method given in [7], the difference being that, in the present paper, the network is accounted for. In section IV, we demonstrate that network effects exhibit a rich interplay with the valve point effect. Therefore, it is important to consider the representation of the valve point effect in future dispatch models. However, the size of the systems considered in the present work renders the approach of [7] non-viable, therefore in this paper we develop a second method. The second method (section III-B) is a local heuristic based on the former approach, and trades optimality guarantees for an acceleration in the computation time. We detail two variants of the heuristic.

A. A globally convergent method

1) Method description: We refer to the globally convergent method proposed in this paper as *APLA*. APLA stands for *adaptive piecewise-linear approximation*. The method starts with a set of knots $\boldsymbol{X}^0$ (red dots in Figs. 1 and 2) satisfying the property described in II-B1, i.e., the inclusion of the kink points in the set of knots. The first surrogate problem, $(S)^0$, which is defined by the first surrogate function, h^0, is then formulated as a mixed-integer problem (MIP) and solved with a predefined tolerance γ. The MIP solver returns a solution, $\boldsymbol{p}^0$, along with a lower bound to the global optimum. The surrogate gap, δ^0, is then computed as,

$$\delta^0 = f(\boldsymbol{p}^0) - h^0(\boldsymbol{p}^0)\,. \quad (11)$$

This gap is visualized in Fig. 1. Then, the optimality gap is computed by adding the solver tolerance and surrogate gap. If the target accuracy is reached, the algorithm stops. Otherwise, the obtained solution $\boldsymbol{p}^0$ is added to the set of knots, refining in this way the approximation, and the algorithm iterates. This process is illustrated in Fig. 2. The red and green dots represent the initial and already added knots, respectively. The purple square is the optimal solution of the surrogate problem and the purple dot is the evaluation of the real objective at this solution. It can be seen that the method locally refines the approximation. In this sense, the method is adaptive and benefits from a lower number of knots with respect to a regular meshing. The efficiency gains of the method rely on quickly converging to a subset of the feasible space where the global optimum should lie. This follows the philosophy of other methods used in dispatch algorithms, such as *stochastic dual dynamic programming (SDDP)* [9], that also aim at computational savings by using locally valid representations of the objective function that is being

optimized, with the purpose of quickly limiting the search to the relevant part of the feasible space by employing the information contained in the approximation of the objective function.

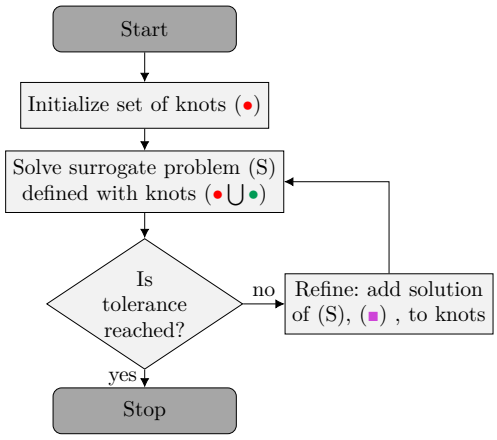

Fig. 2. Flow chart of the method APLA.

2) Convergence guarantees: At iteration k of the method, the optimality gap can be computed as [7]

$$f(\boldsymbol{p}^k) - f(\boldsymbol{p}^*) \leq \overbrace{\delta^k + \gamma^k + \epsilon^k}^{\text{Optimality gap}}, \tag{12}$$

where $\boldsymbol{p}^*$ is the optimal solution of (P), γ^k stands for the gap of $(S)^k$ returned by the MIP solver, and ϵ^k is an over-approximation error. This over-approximation error is almost equal to zero for the cost functions considered here (see [7]), hence we will neglect it in the rest of the paper. The following result, given in [7], also still holds because it only relies on the Lipschitz continuity of the objective functions and on the boundedness of the feasible set.

Theorem 1. *For Lipshitz continuous cost function f, the sequence of iterations provided by APLA satisfies*

$$\lim_{k\to\infty} \delta^k = 0\,.$$

3) Stopping criterion: The algorithm terminates when the optimality gap, eq. (12), is lower than a predefined tolerance γ: $\delta^k + \gamma^k \leq \gamma$. This γ is chosen to be equal to the targeted MIP gap, i.e., the gap between the lower and upper objective bound of the surrogate problem, which is given as input to the MIP solver. Theorem 1 shows that the method converges but the drawback is that the method requires several costly calls to the MIP solver, which increase the computation time of the algorithm. This motivates the development of a heuristic, described in the following section, as well as a time criterion based on the number of iteration and the maximum time allowed to the MIP solver. This time criterion is also used in the experiments section IV.

B. A local heuristic

1) Method description: Fig. 3 summarizes the heuristic which can be split into two steps: first a global search is made on the whole feasible set in order to find optimum candidates. Then, the search is refined around these candidates. In [10], the authors proposed to use the solution of the initial surrogate problem as the initial point of an interior point method. Here, we follow the same approach with three main differences: a) the initial point is obtained with a few steps of APLA, b) a list of candidates is considered and c) the local search method is also based on a local approximation. Let us explain more formally these three points.

a) Search for an initial point: The first step of this heuristic is to select a promising candidate, around which the local search will be initialized. In order to achieve this, the APLA algorithm is used with a finite number of iterations, n_{iter}, over the whole search space Ω, i.e., the feasible set of (P). This number is typically chosen to be very small to avoid excessive running time. In the experiments below, we take $n_{\text{iter}} = 2$.

b) List of candidates: During the search for an initial point, several potential candidates for the global solution of the surrogate problems are found by the MIP solver. Most of these points, called *incumbents*, are good initial guesses for a local search. Hence, APLA is slightly modified to return a list $\mathcal{L}_{\text{I}}$ of the best incumbents, which will serve as initial guesses. Using a list of initial guesses instead of a single starting point reduces the sensitivity of the method with respect to the initial point.

c) Local search method: The local search in the neighbourhood $\Omega_{\tilde{\boldsymbol{p}}^i}$, of a specific point $\tilde{\boldsymbol{p}}^i$, at iteration i of the inner loop, proceeds as follows: the power generation constraint of eq. (6) is narrowed around the value $\tilde{\boldsymbol{p}}^i$ via the closest knots. Eq. (6) now reads

$$X^i_{gtj} \leq p_{gt} \leq X^i_{gtj'} \tag{13}$$

for $j < j'$ and $X^i_{gtj} \leq \tilde{p}^i_{gt} \leq X^i_{gtj'}$. In this way, the feasible set is strongly reduced and the power ranges become $t-$dependent. In the specific case when $j' = j+1$, the (first) local problem becomes a much simpler convex quadratic problem which can be solved efficiently.

2) Convergence guarantees: This APLA-based is converging because every APLA call inside the loop (Fig. 3) converges by theorem 1, and the number of loop calls is equal to the finite size of $\mathcal{L}_{\text{I}}$. However, the lower bound obtained on sub-instance $\Omega_{\tilde{\boldsymbol{p}}^i}$ is not a lower bound for (P). As we neglect the over-approximation error, the optimality gap is computed as follows,

$$f(\boldsymbol{p}^{i,\tilde{k}}) - f(\boldsymbol{p}^*) \leq \overbrace{f(\boldsymbol{p}^{i,\tilde{k}}) - \left(h^{n_{\text{iter}}}(\boldsymbol{p}^{n_{\text{iter}}}) - \gamma^{n_{\text{iter}}}\right)}^{\text{Optimality gap}}, \tag{14}$$

where $(\boldsymbol{p}^{i,\tilde{k}})_{\tilde{k}=0,\,1\ldots}$ and $(\boldsymbol{p}^k)_{k=0,1,\ldots,n_{\text{iter}}}$ are the sequences of solutions from $\text{APLA}(\Omega_{\tilde{\boldsymbol{p}}^i}, \infty)$ and $\text{APLA}(\Omega, n_{\text{iter}})$. Eq. 14 shows that once the heuristic enters the inner loop

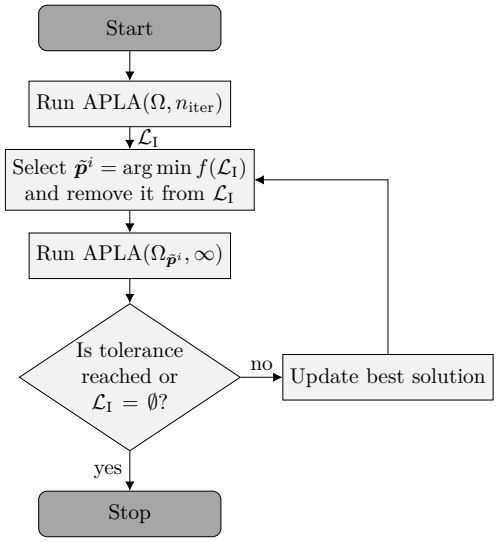

Fig. 3. Flow chart of the APLA-based heuristic.

in Fig. 3, it reduces the optimality gap only by decreasing the objective.

An expression similar to eq. (12) can also be obtained,

$$\begin{aligned} f(\boldsymbol{p}^{i,\tilde{k}}) - f(\boldsymbol{p}^*) &\leq f(\boldsymbol{p}^{i,\tilde{k}}) - (h^{n_{\text{iter}}}(\boldsymbol{p}^{n_{\text{iter}}}) - \gamma^{n_{\text{iter}}}), \\ &= f(\boldsymbol{p}^{i,\tilde{k}}) - f(\boldsymbol{p}^{*,i}) + \gamma^{n_{\text{iter}}} \\ &+ \underbrace{f(\boldsymbol{p}^{*,i}) - h^{n_{\text{iter}}}(\boldsymbol{p}^{n_{\text{iter}}})}_{:=\zeta^i}, \\ &\leq \delta^{i,\tilde{k}} + \gamma^{i,\tilde{k}} + \epsilon^{i,\tilde{k}} + \gamma^{n_{\text{iter}}} + \zeta^i, \\ &\approx \delta^{i,\tilde{k}} + \gamma^{n_{\text{iter}}} + \zeta^i, \end{aligned} \tag{15}$$

where $\boldsymbol{p}^{*,i} := \arg\min_{\boldsymbol{p} \in \Omega_{\tilde{\boldsymbol{p}}^i}} f(\boldsymbol{p})$. The second inequality holds because the application of APLA on the restricted domain $\Omega_{\tilde{\boldsymbol{p}}^i}$ is a valid instance. Hence, eq. (12) can be used. Furthermore, the over-approximation error is negligible here and the restricted instances APLA($\Omega_{\tilde{\boldsymbol{p}}^i}, \infty$) are solved to optimality, i.e., with a tolerance $\gamma^{i,\tilde{k}} \approx 0$.

Eq. 15 shows that at iteration $\tilde{k}$ of APLA($\Omega_{\tilde{\boldsymbol{p}}^i}, \infty$), there are three main contributions to the optimality gap. Firstly, $\delta^{i,\tilde{k}}$, which is the gap between the surrogate and true function. This gap goes to zero as $\tilde{k}$ goes to ∞ by Theorem 1. Secondly, $\gamma^{n_{\text{iter}}}$, the MIP gap obtained at the end of APLA(Ω, n_{iter}) and finally, ζ_i, which captures the fact that the optimal solution $\boldsymbol{p}^*$ may lie outside of $\Omega_{\tilde{\boldsymbol{p}}^i}$.

By construction $\boldsymbol{p}^{n_{\text{iter}}} \in \mathcal{L}_{\text{I}}$, and in the special case where $\tilde{\boldsymbol{p}}^i = \boldsymbol{p}^{n_{\text{iter}}}$, we have $f(\boldsymbol{p}^{*,i}) \leq f(\boldsymbol{p}^{n_{\text{iter}}})$, which implies that $\zeta^i \leq \delta^{n_{\text{iter}}}$: the heuristic either improves $\boldsymbol{p}^{n_{\text{iter}}}$ or shows that it is globally optimal.

3) Stopping criterion: The heuristic terminates either if it reaches the targeted optimality gap, eq. (14), or after iteration over the whole list $\mathcal{L}_{\text{I}}$.

4) Extension of the methods: Similarly as APLA, the heuristic can be easily extended to account for spinning reserves, multiple fuels, and prohibited operation zones (POZ). This will incur an increase in the number of integer variables and further motivate the use of an APLA-based heuristic.

IV. Test case study

In this section, the comparison is made between the two approaches detailed in section III and the benefit from taking the VPE into account is estimated. In this work, Gurobi 8.1 [11] has been used for solving the MIP problem associated with the surrogate problem. The optimization has been run on a computer with Intel-i7 3.6 GHz CPU and 16 GB of RAM. Two variants of the heuristic from section III-B are tested: H-local, which restricts the feasible region to a single segment, i.e., $j' = j+1$ from eq. (13), and H-full, which restricts the feasible region to up to three segments. The impact of the VPE is highlighted by comparing the solution obtained via the aforementioned methods with respect to the solution from a method which does not take the VPE into account.

The data and algorithm implementations are available on GitLab [12].

A. Data set creation

As no data set with transmission constraints and VPE is openly available in the literature, we analyse the IEEE test systems, by introducing additional generators that obey VPE. We use IEEE test system data from the PSTCA and MatPower ([13], [14]), while VPE generator data can be found in [15]. The VPE generators are added randomly in buses of the IEEE networks which are represented in Figs. 4 and 7. In order to limit the uncertainty from this random selection, 100 trials of the algorithm are made with different network configurations. This allows for a more robust analysis of the methods. We further assess the scalability of the method by increasing the number of VPE units. In particular, we double the number of VPE units, and introduce a 5% variation on the parameters of these VPE units. We include this variation in order to avoid symmetry, which creates unnecessary computational complexity, since it is rarely the case that different physical assets share an identical set of economic and technical parameters. We denote as *experiment* the simulation of 100 different *instances* of the problem.

B. IEEE cases with 10 added VPE units

1) IEEE 57-bus system: The original case study with seven generators [13] is extended by including ten additional generators that obey a valve point effect. The network topology is sketched in Fig. 4. The tolerance of the MIP solver and the maximal MIP solver time are set to 0.1% and 45 seconds when the surrogate problem is defined over the whole domain Ω, and to 0.01% and 45 seconds when the problem is restricted to a subdomain $\Omega_{\tilde{\boldsymbol{p}}^i}$. Figs. 5 and 6 (blue boxes) present a comparison between the execution time and the final optimality gap of the three methods: H-full, H-local and APLA. Whereas some instances of the initial APLA algorithm can be

resolved in a few seconds, others require significantly more time, due to timeouts. The timeout limit for APLA is set at a maximum of ten iterations of 45 seconds.

The two heuristics, H-full and H-local, perform much faster, and the majority of instances is executed within 20 seconds (H-local) and 100 seconds (H-full). This time improvement is at the cost of an increase in the optimality gap, with about half of the instances being solved at the target tolerance of 0.1%. The bottom magnification in Fig. 5 shows that the median execution time of H-local is approximately four times lower than the median of H-full, while the optimality gap, depicted in Fig. 6, is comparable. We discuss the implication of these observations in detail in section IV-E.

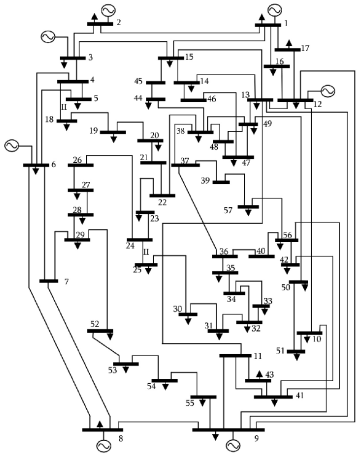

Fig. 4. Single-line diagram of IEEE 57 bus system [16].

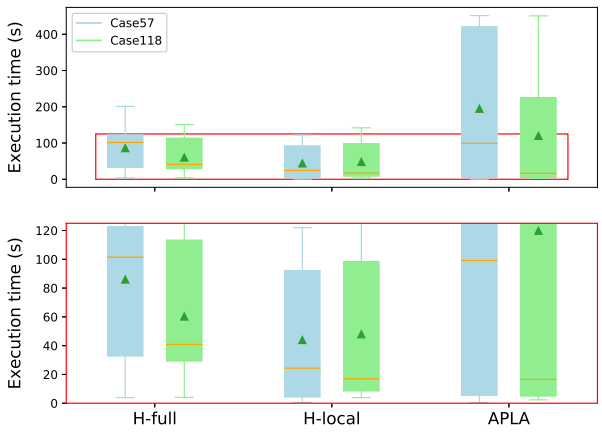

Fig. 5. Comparison between the execution time of the methods for 100 random instances with targeted optimality gap of 0.1%. The orange lines and green triangles represent the medians and means, respectively. The bottom frame is a magnification of the upper one.

2) IEEE 118-bus system: In a similar way as the previous case, we extended the 54-generator IEEE 118-bus system (Fig. 7) with the same ten generators obeying a valve point effect [13]. Tests are performed with the same methods and parameters as in section IV-B1. The comparison of the execution time, Fig. 5 (green boxes), shows that APLA performs faster in the IEEE 118 case but it is still outperformed by the two heuristics. However, the final optimality gap (Fig. 6) and final objective (table I) is slightly better with APLA. We discuss the implication of these results in detail in section IV-E.

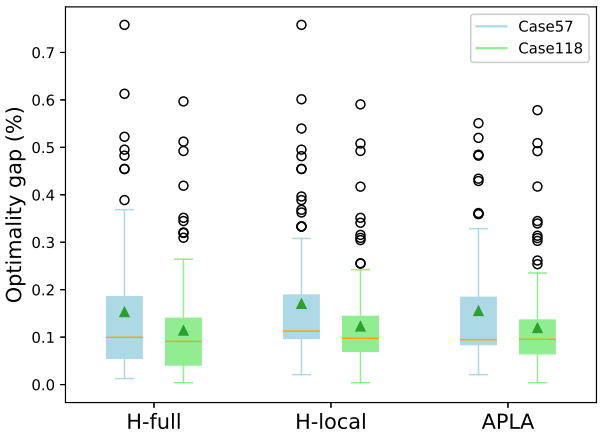

Fig. 6. Comparison between the final optimality gap of the methods proposed in the paper for 100 random instances with targeted optimality gap of 0.1%.

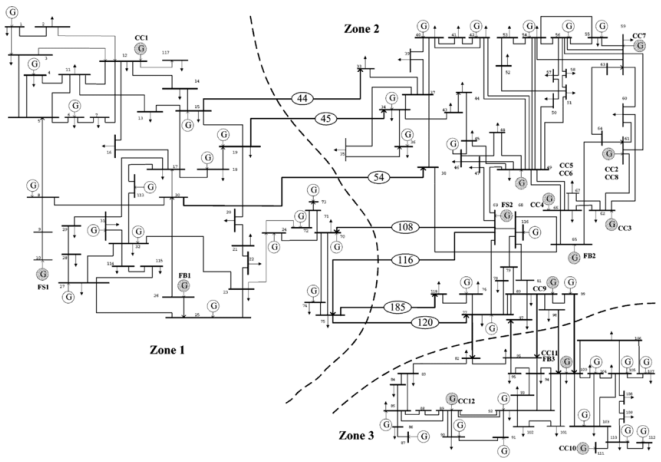

Fig. 7. Single-line diagram of IEEE 118 bus system [17].

C. IEEE cases with 20 added VPE units

As observed in the previous section, increasing the size of the network while keeping the number of VPE units constant does not pose significant computational complications. On the contrary, a larger network may result in reduced run times. In this section, we increase the size of the problem by adding ten additional VPE units to the systems.

1) IEEE 57-bus system: We perform tests on an extension of the 57-bus case using the same methods and parameters as in section IV-B1. We report the results in

Figs. 8 and 9. Compared to the previous tests, all three methods exhibit a similar relative increase in run time and final optimality gap. However, the absolute values of the running time and optimality gap remain acceptable for real time applications. The performance of the methods relative to each other is similar to that of the previous case, and the discussion is then analogous to section IV-B1.

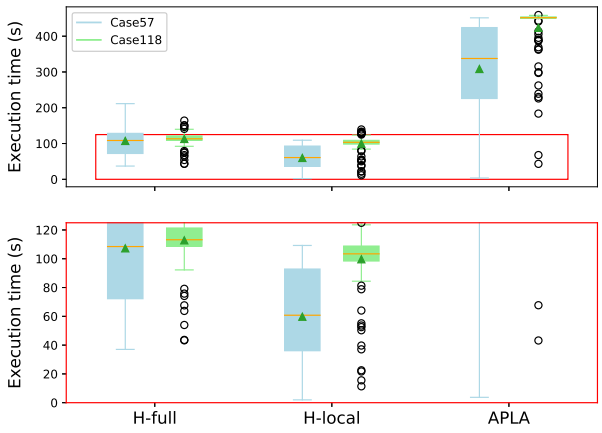

Fig. 8. Comparison between the execution time of the methods for 100 random instances of IEEE test cases with 20 additional VPE units and a targeted optimality gap of 0.1%.

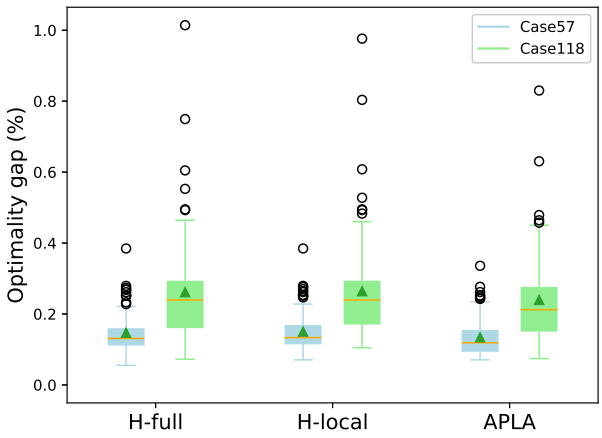

Fig. 9. Comparison between the final optimality gap of the methods for 100 random instances with 20 additional VPE units and a targeted optimality gap of 0.1%.

2) IEEE 118-bus system: We perform tests on an extension of the 118-bus case using the same methods and parameters as in section IV-B1. In this case, the median final optimality gap doubles. However, the heuristics still outperform APLA execution time and the difference between both heuristics is reduced, with a faint dominance of H-local. Further comments on this increase are made in section IV-E.

D. Impact of the VPE

In order to assess the benefit of accounting for the VPE, each instance of both case studies is solved, while ignoring the VPE, by specifically removing the rectified sine term. As a result of this simplification, the objective function becomes quadratic and the problem becomes much simpler. The computation time is less than a second, but there is no guarantee with respect to the optimal solution. The mean of the final objective is reported in table I, for this method (QP) as well as for APLA and both heuristics. The cost of neglecting the VPE can be readily estimated at 5% and 1% for the IEEE 57 and IEEE 118-bus system case with 10 additional VPE units, respectively. The second experiment, including 20 additional VPE units, shows larger discrepancies with 8% and 3.3% differences.

TABLE I
OBJECTIVE MEAN OF EACH METHOD.

	H-full	H-local	APLA	QP
Case57 (10 VPE-units)	621622	621634	**621547**	654535
Case118 (10 VPE-units)	2447475	2447540	**2447383**	2471132
Case57 (20 VPE-units)	587695	587713	**587669**	634653
Case118 (20 VPE-units)	2227536	2227592	**2227087**	2301490

E. Discussion

The application of the APLA method on a network-constrained case study is compromised by the fact that a significant number of instances terminate due to timeouts. These timeouts push up the mean of the execution time. However, the heuristics based on the former method are able to reach at least 0.3% optimality gap for 75% of the instances in reduced time, relatively to APLA.

Also, APLA reduces the optimality gap by increasing the lower bound, on the one hand, and by decreasing the optimal objective, on the other hand. On the contrary, the heuristic approaches compute a single lower bound and then focus on the objective; for the same optimality gap, the solution of the heuristic is therefore lower. This phenomenon is highlighted by the fact that even if the final optimality gap depicted in Figs. 6 and 9 is approximately 10% better for APLA, the final APLA objective reported in table I is lower than the heuristics by only $\sim 0.01\%$ on average. Of the two variants of the heuristic considered, H-local, which restricts the local search on a smaller subset than H-full, performs slightly faster.

The scalability of the method is assessed in two stages. Firstly, the number of buses and generators is increased, while keeping the number of VPE units constant, and then this number is doubled. The first experiments (Figs. 5 and 6) have shown that the problem does not become more difficult when increasing the number of nodes and usual thermal units; the problem becomes even easier when the number of nodes is increased from 57 to 118. The second experiments (Figs. 8 and 9) show that this is

not always true: with 20 additional VPE units, the 57-bus system becomes easier than the 118-bus system. In general, the execution time increases and the quality of the solution worsens when increasing the number of VPE units. However, despite this time and gap increase, the values of these quantities remain under two minutes and 0.25 %, respectively, for most instances.

As shown in the experiments, the core difficulty of the problem lies rather in the number of VPE units than in the total number of units. This motivates the application of the heuristics on real test cases where only a small fraction of the units obeys a valve point effect.

Finally, the cost of the valve point effect computed for both test cases demonstrates the interplay of the network with the VPE; ignoring the VPE costs on average 5% for the 57-bus case and 1% for the 118-bus case. This difference can be explained by the distinct level of VPE-units in the two test cases: more than half of the units obey a valve point effect for the modified IEEE 57 case, while this number is reduced to fifteen percent in the second case. These numbers increase for the case with 20 additional VPE units. The average relative cost of neglecting the VPE units is estimated at 8% and 3% for the 57-bus and 118-bus case, respectively.

V. Conclusion

In this paper, a global method for the solution of the multi-period economic dispatch problem with transmission constraints has been studied. This method, the adaptive piecewise-linear approximation (APLA), suffers from long execution time when applied to larger problems with network constraints, and a ten-minute run time threshold (which is a reasonable upper bound on economic dispatch models in European market operations) is attained several times. This motivates the development of a faster method, which still targets the global solution of this non-convex problem and provides guarantees with respect to the final solution.

Our main contributions are i) to demonstrate that VPE *matters* in test instances with network constraints and ii) to develop local heuristics which accelerate the execution time of the problem.

The APLA method, as well as the heuristics, are tested on several instances of the IEEE 57-bus and IEEE 118-bus system. We show that the heuristics produce solutions of comparable quality to those obtained by APLA, at a fraction of the computation time required by the latter. The additional cost of ignoring the VPE effect is computed for the different instances of the two IEEE systems and is measured on average as up to eight percent.

Further work may include the extension of the method to unit commitment and an analysis of the interactions of the valve point effect with the scheduling decisions. The impact of the position of the VPE-units in the network may also be of interest, as suggested by the various range of solutions obtained here for different network topologies. With the aim of improving the practicality of the model, some direct extensions could be contemplated. Firstly, the method presented here can be adapted to account for quadratic power losses, through a piecewise relaxation of the losses. Secondly, a more realistic power flow model, such as a convex ACOPF, could also be used. The main change would be to resort to a mixed-integer second order cone programming (MISOCP) solver instead of a MIP one.

Acknowledgment

This work was supported by the Fonds de la Recherche Scientifique - FNRS under Grant no. PDR T.0025.18.

References

[1] G. L. Decker and A. D. Brooks, "Valve point loading of turbines," *Electrical Engineering*, vol. 77, no. 6, pp. 501–501, Jun. 1958.

[2] K. P. Wong and C. C. Fung, "Simulated annealing based economic dispatch algorithm," *IEEE Proceedings C - Generation, Transmission and Distribution*, vol. 140, no. 6, pp. 509–515, Nov 1993.

[3] L. S. Coelho and V. C. Mariani, "Combining of chaotic differential evolution and quadratic programming for economic dispatch optimization with valve-point effect," *IEEE Transactions on power systems*, vol. 21, no. 2, pp. 989–996, 2006.

[4] M. J. Mokarram, T. Niknam, J. Aghaei, M. Shafie-khah, and J. P. Catalao, "Hybrid optimization algorithm to solve the non-convex multiarea economic dispatch problem," *IEEE Systems Journal*, 2019.

[5] T. Niknam, M. R. Narimani, and R. Azizipanah-Abarghooee, "A new hybrid algorithm for optimal power flow considering prohibited zones and valve point effect," *Energy Conversion and Management*, vol. 58, pp. 197 – 206, 2012.

[6] P. A. Absil, B. Sluysmans, and N. Stevens, "MIQP-based algorithm for the global solution of economic dispatch problems with valve-point effects," in *2018 Power Systems Computation Conference (PSCC)*, June 2018, pp. 1–7.

[7] L. Van Hoorebeeck, A. Papavasiliou, and P.-A. Absil, "MILP-based algorithm for the global solution of dynamic economic dispatch problems with valve-point effects," *IEEE Power and Energy Society General Meeting*, 2019.

[8] D. Walters and G. Sheble, "Genetic algorithm solution of economic dispatch with valve point loading," *IEEE Transactions on Power Systems*, vol. 8, no. 3, pp. 1325–1332, Aug. 1993.

[9] M. V. F. Pereira and L. M. V. G. Pinto, "Multi-stage stochastic optimization applied to energy planning," *Mathematical Programming*, vol. 52, no. 1, pp. 359–375, May 1991.

[10] S. Pan, J. Jian, and L. Yang, "A hybrid MILP and IPM approach for dynamic economic dispatch with valve-point effects," *International Journal of Electrical Power & Energy Systems*, vol. 97, pp. 290 – 298, 2018.

[11] Gurobi Optimization Inc, "Gurobi Optimizer Reference Manual," 2018. [Online]. Available: http://www.gurobi.com

[12] L. Van Hoorebeeck, "Adaptive piecewise approximation," https://gitlab.com/Loicvh/apla, 2019.

[13] R. D. Christie, "Power systems test case archive," 1999, accessed: 2019-08-07. [Online]. Available: http://labs.ece.uw.edu/pstca

[14] R. D. Zimmerman and C. E. Murillo-Sanchez, "Matpower (version 7.0)," https://matpower.org.

[15] P. Attaviriyanupap, H. Kita, E. Tanaka, and J. Hasegawa, "A hybrid EP and SQP for dynamic economic dispatch with nonsmooth fuel cost function," *IEEE Transactions on Power Systems*, vol. 17, no. 2, pp. 411–416, May 2002.

[16] A. R. Al-Roomi, "Power Flow Test Systems Repository," Halifax, Nova Scotia, Canada, 2015. [Online]. Available: https://al-roomi.org/power-flow

[17] B. Lu and M. Shahidehpour, "Unit commitment with flexible generating units," *Power Systems, IEEE Transactions on*, vol. 20, pp. 1022 – 1034, 06 2005.